

### Ⅲ. 研究成果の刊行に関する一覧表

## 研究成果の刊行に関する一覧表

### 雑誌

1. Rafei D, Müller R, Ishii N, Llamazares M, Hashimoto T, Hertl M, Eming R: IgG autoantibodies against desmocollin 3 in pemphigus sera induce loss of keratinocyte adhesion. *Am J Pathol* 178(2):718-723, 2011.
2. Ishigami T, Kubo Y, Matsudate Y, Ansai S, Arase S, Ohyama B, Hashimoto T. Pananeoplastic pemphigus associated with non-Hodgkin's lymphoma. *Eur J Dermatol* 21(1):122-124, 2011.
3. Abreu-Verez AM, Howard MS, Yi H, Gao W, Hashimoto T, Grossiklaus HE: Neural system antigens are recognized by autoantibodies from patients affected by a new variant of endemic pemphigus foliaceus in Colombia. *J Clin Immunol* 31(3):356-368, 2011.
4. Prado R, Brice SL, Fukuda S, Hashimoto T, Fujita M. Paraneoplastic pemphigus herpetiformis with IgG antibodies to desmoglein 3 and without mucosal lesions. *Arch Dermatol* 147(1):67-71, 2011.
5. Choi Y, Lee SE, Fukuda S, Hashimoto T, Kim SC. Mucous membrane pemphigoid with immunoglobulin G autoantibodies against full-length and 120-kDa ectodomain of BP180. *J Dermatol* 38(2):169-172, 2011.
6. Dainichi T, Hirakawa Y, Ishii N, Ohyama B, Kohda F, Takahara M, Moroi Y, Furue M, Yasumoto S, Hashimoto T: Mucous membrane pemphigoid with autoantibodies to all the laminin 332 subunits and fatal outcome resulting from liver cirrhosis and hepatocellular carcinoma. *J Am Acad Dermatol* 64 (6):1199-1200, 2011.
7. Csorba K, Schmidt S, Florea F, Ishii N, Hashimoto T, Hertl M, Karpati S, Bruckner-Tuderman L, Nishie W, Sitaru C. Development of an ELISA for sensitive and specific detection of IgA autoantibodies against BP180 in pemphigoid diseases. *Orphanet J Rare Dis* 6(1):31, 2011.
8. Tsuruta D, Ishii N, Hamada T, Ohyama B, Fukuda S, Koga H, Imamura K, Kobayashi H, Karashima T, Nakama T, Dainichi T, Hashimoto T. IgA pemphigus. *Clin Dermatol* 29(4):437-442, 2011.

9. Davis RF, Ravenscroft J, Hashimoto T, Evans JH, Harman KE. Bullous pemphigoid associated with renal transplant rejection. *Clin Exp Dermatol*. 36(7):824-825, 2011.
10. Hashimoto T, Tsuruta D, Dainichi T, Hamada T, Furumura M, Ishii N. Demonstration of epitope spreading in bullous pemphigoid: results of a prospective multicenter study. *J Invest Dermatol* 131(11):2175-2177, 2011.
11. Arakawa M, Dainichi T, Ishii N, Hamada T, Karashima T, Nakama T, Yasumoto S, Tsuruta D, Hashimoto T. Lesional Th17 cells and regulatory T cells in bullous pemphigoid. *Exp Dermatol* 20(12):1022-1024, 2011.
12. Fukuda S, Tsuruta D, Uchiyama M, Mitsuhashi Y, Kobayashi H, Ishikawa T, Ohyama B, Ishii N, Hamada T, Dainichi T, Karashima T, Nakama T, Yasumoto S, Hashimoto T. Brunsting-Perry type pemphigoid with IgG autoantibodies to laminin-332, BP230 and desmoplakins I/II. *Br J Dermatol*. 165(2):433-435, 2011.
13. Murrell DF, Daniel BS, Joly P, Borradori L, Amagai M, Hashimoto T, Caux F, Marinovic B, Sinha AA, Hertl M, Bernard P, Sirois D, Cianchini G, Fairley JA, Jonkman MF, Pandya AG, Rubenstein D, Zillikens D, Payne AS, Woodley D, Zambruno G, Aoki V, Pincelli C, Diaz L, Hall RP, Meurer M, Mascaro JM Jr, Schmidt E, Shimizu H, Zone J, Swerlick R, Mimouni D, Culton D, Lipozencic J, Bince B, Bystryr JC, Werth VP. Definitions and outcome measures for bullous pemphigoid: Recommendations by an international panel of experts. *J Am Acad Dermatol*. 66(3):479-485, 2011.
14. Kiniwa Y, Ashida A, Ohashi A, Kitoh R, Fukuda S, Hashimoto T, Okuyama R. A case of epidermolysis bullosa acquisita associated with laryngeal stenosis. *Acta Derm Venereol*. 92(1):93-4, 2012.
15. Monshi B, Richter L, Hashimoto T, Groß E, Haensch N, Rappersberger K. IgA pemphigus of the subcorneal pustular dermatosis type : Successful therapy with a combination of dapsone and acitretin. *Hautarzt*. 2012 Jan 6. (German) PMID: 22218566 [Epub ahead of print]
16. Koga H, Ohyama B, Tsuruta D, Ishii N, Hamada T, Dainichi T, Natsuaki Y, Sogame R, Fukuda S, Karashima T, Tada J, Yamashiro M, Uezato H, Chan PT, Hashimoto T. Five Japanese cases of anti-Dsg1 antibody positive and anti-Dsg3 antibody negative pemphigus with oral lesions. *Br J Dermatol*. 2012 Jan 13. doi: 10.1111/j.1365-2133.2012.10827.x. [Epub ahead of print]

17. Ohyama B, Nishifuji K, Chan PT, Kawaguchi A, Yamashita T, Ishii N, Hamada T, Dainichi T, Koga H, Tsuruta D, Amagai M, Hashimoto T. Epitope Spreading Is Rarely Found in Pemphigus Vulgaris by Large-Scale Longitudinal Study Using Desmoglein 2-Based Swapped Molecules. *J Invest Dermatol*. 132(4):1158-68, 2012.
18. Karashima T, Tsuruta D, Hamada T, Ishii N, Ono F, Hashikawa K, Ohyama B, Natsuaki Y, Fukuda S, Koga H, Sogame R, Nakama T, Dainichi T, Hashimoto T. Interaction of plectin and intermediate filaments. *J Dermatol Sci*, 66(1):44-50, 2012.
19. Komorowski L, Muller R, Vorobyev A, Probst C, Recke A, Jonkman MF, Hashimoto T, Kim SC, Groves R, Ludwig RJ, Zillikens D, Stocker W, Schmidt E. Sensitive and specific assays for routine serological diagnosis of epidermolysis bullosa acquisita. *J Am Acad Dermatol*, 2012 Feb 15. PMID: 22341608 [Epub ahead of print]

#### IV. 研究成果の刊行物・別刷

## IgG Autoantibodies Against Desmocollin 3 in Pemphigus Sera Induce Loss of Keratinocyte Adhesion

David Rafei,\* Ralf Müller,\* Norito Ishii,†  
Maria Llamazares,\* Takashi Hashimoto,†  
Michael Hertl,\* and Rüdiger Eming\*

From the Department of Dermatology and Allergology,\* Philipps University, Marburg, Germany; and the Department of Dermatology,† Kurume University School of Medicine, Fukuoka, Japan

**Pemphigus is considered an autoimmune bullous skin disorder associated with IgG against the desmosomal components, desmoglein 3 (Dsg3) and desmoglein 1 (Dsg1). This concept is supported by the *in vitro* and *in vivo* pathogenicity of anti-Dsg3/Dsg1 IgG and the mucosal blistering phenotype of mice with a genetic deficiency of Dsg3. Mice deficient for another desmosomal adhesion molecule, desmocollin 3 (Dsc3), show a similar pemphigus phenotype, and we investigated the pathogenicity of Dsc3-reactive IgG autoantibodies that were identified previously in a subset of patients with atypical pemphigus. We here demonstrate that IgG against Dsc3 causes loss of adhesion of epidermal keratinocytes. Specifically, IgG against Dsc3 was purified from Dsc3-reactive pemphigus sera by affinity column chromatography using recombinant human Dsc3. Affinity purified IgG was functionally active and did not only react with recombinant Dsc3 but also with epidermis and cultured human keratinocytes. Moreover, Dsc3-reactive IgG induced loss of adhesion of epidermal keratinocytes in a dispase-based keratinocyte dissociation assay that was reversed on pre-adsorption with human Dsc3 but not Dsg3. These findings demonstrate that IgG autoantibodies against an additional component of the desmosomes, Dsc3, induce loss of keratinocyte adhesion and thus may contribute to blister formation in pemphigus. (*Am J Pathol* 2011, 178:718–723; DOI: 10.1016/j.ajpath.2010.10.016)**

Pemphigus is a severe autoimmune bullous disorder of mucous membranes and skin which has been associated with autoantibodies (autoab) of the IgG class against two desmosomal components of epidermal keratinocytes, desmoglein 1 (Dsg 1) and desmoglein 3 (Dsg3).<sup>1,2</sup> Distinct clinical pemphigus variants, such as pemphigus vulgaris (PV) and pemphigus foliaceus (PF) have been linked to the presence of IgG reactive with their specific target antigens, Dsg3 and Dsg1, respectively.<sup>3</sup> Moreover, the clinical phenotype of these pem-

phigus variants can be largely explained by the tissue expression pattern of their autoantigens.<sup>4</sup> PV is characterized by suprabasal loss of adhesion of the mucous membranes, the site where Dsg3 is predominantly expressed.<sup>5</sup> In contrast, PF is recognized by superficial blisters of the skin but not of the mucosa because Dsg1 is preferentially produced by the subcorneal epidermis of stratified epithelia such as the skin.

In addition to the presence of four desmosomal Dsg isoforms, ie, Dsg1-4, epidermal desmosomes contain three different isoforms of another group of cadherins, namely desmocollin 1 (Dsc 1), desmocollin 2 (Dsc 2), and desmocollin 3 (Dsc 3).<sup>6,7</sup> Dsc1 has been previously identified as the target antigen of IgA autoab in the subcorneal pustular dermatosis type of IgA pemphigus.<sup>8</sup> Moreover, IgG autoab against Dsc1, Dsc2, or Dsc3 were detected in the sera of patients with paraneoplastic pemphigus and, occasionally, in patients with atypical pemphigus.<sup>9–12</sup> However, the pathogenic relevance of Dsc-specific autoab in these disorders remains unclear.

The concept that the pathogenesis of pemphigus is exclusively linked to IgG autoab against Dsg1 and Dsg3 has been challenged by the recent observation that mice with a genetic deficiency of Dsc3 show a pronounced blistering phenotype with suprabasal loss of epidermal adhesion that is highly reminiscent of PV.<sup>13</sup> It has been reported that Dsc3, as Dsg3, is preferentially expressed in the basal and suprabasal layers of human epidermis the site where loss of adhesion occurs in PV.<sup>6,7,13</sup> Dsg1 and Dsg3 not only interact in desmosomes via homophilic transinteraction, but presumably also interact by heterophilic binding with Dsc isoforms such as Dsc1 and Dsc3. However, an heterophilic transinteraction between Dsg3 and Dsc3 is unlikely based on recent *in vitro* findings.<sup>14</sup>

Supported by the German Research Council (Deutsche Forschungsgemeinschaft, He1602/8-1; 8-2 to M.H.) through the Coordination Theme 1 (Health) of the European Community's FP7, Grant agreement number HEALTH-F2- 2008-200515 (M.H.); and by the Federal Ministry for Education and Research (BMBF; Nr. 01GN0973 to M.H. and R.E.).

M.H. and R.E. contributed equally to this work.

Accepted for publication October 21, 2010.

Current address of R.M.: Department of Dermatology, Venerology and Allergology, University of Lübeck, Germany.

Address reprint requests to: Rüdiger Eming, M.D., or Michael Hertl, M.D., Ph.D., Department of Dermatology and Allergology, Philipps University, Deutschhausstrasse 9, D-35033 Marburg, Germany. E-mail: eming@med.uni-marburg.de or hertl@med.uni-marburg.de.

**Table 1.** Autoantibody Profile and Clinical Characteristics of the Studied Pemphigus Patients

Patient	Autoab isotype	Diagnosis	Clinical characteristics	Desmosomal target antigens*				
				Dsc1	Dsc2	Dsc3	Dsg1	Dsg3
1	IgG	Pemphigus vegetans	Exophytic skin erosions and oral erosions	-	-	+	-	-
2	IgG	Pemphigus vegetans	Hypertrophic verrucous plaques with pustules and erosions on foot, groin, and scalp	-	-	+	+	-
3	IgG	Pemphigus herpetiformis	Multiple pustules, erythematous herpetiform erosions, oral erosions	-	-	+	-	-
4	IgG	Pemphigus herpetiformis	Erythematous cutaneous erosions	-	-	+	-	-

Autoab, autoantibody; Dsc, desmocollin; Dsg, desmoglein.

\*Serum IgG reactivity as determined by immunoblot analysis using recombinant Dsg and Dsc proteins (see Figure 2).

In the present study, affinity-purified, Dsc3-reactive IgG fractions from pemphigus sera induced loss of epidermal keratinocyte adhesion in a similar manner as pathogenic anti-Dsg3 IgG autoab. Thus, Dsc3 can be considered as a relevant autoantigen of pemphigus and Dsc3-reactive IgG autoab may contribute to the blistering phenotype of pemphigus.

## Materials and Methods

### Patients

Sera of four patients with atypical pemphigus (pemphigus vegetans and pemphigus herpetiformis) were investigated. Assessment of the clinical conditions revealed exophytic skin erosions of the fingers and oral erosions (patient 1), hypertrophic vegetative (verrucous) plaques with pustules and erosions on the foot, groin, and scalp (patient 2), widespread erythema, pustules, and erosions of the oral mucosa (patient 3) and multiple erythematous erosions on trunk and extremities (patient 4). The clinical diagnosis of pemphigus was confirmed by: (a) histopathological evidence of intraepidermal loss of adhesion; (b) IgG deposits on the surface of epidermal keratinocytes of perilesional skin by direct immunofluorescence; and (c) cell surface IgG reactivity on monkey esophagus epithelium by indirect immunofluorescence. The clinical and immunoserological characteristics of the patients are shown in Table 1. Except for patient 2, who also had Dsg1-reactive IgG, all of the other patients predominantly demonstrated IgG reactivity to Dsc3. Figure 1 depicts representative clinical pictures of the studied patients. All patients gave written consent to participate in this investigation, which adhered to the Declaration of Helsinki Guidelines and was approved by the local ethics committee.

### Recombinant Dsc and Dsg Proteins

The recombinant Dsc and Dsg proteins were expressed in insect cells (High Five; Invitrogen, Carlsbad, CA) by infection with recombinant baculovirus as previously described<sup>9,15</sup> (Figure 2A). Culture supernatants of infected cells were collected after 3 days and recombinant proteins were purified by affinity chromatography using nickel-nitrilotriacetic-linked agarose beads (Qiagen, Hilden, Germany) according to the manufac-

turer's instructions. Purified proteins were gradually dialyzed against phosphate-buffered saline (PBS) supplemented with 0.5 mmol/L CaCl<sub>2</sub> and stored at -20°C. By immunoblot analysis, the purified recombinant proteins displayed the expected size and were specifically immunoreactive using a monoclonal mouse anti-Etag antibody (1:1000; Amersham, Biosciences, Uppsala, Sweden) (Figure 2B, upper panel). In addition, serum of a patient with paraneoplastic pemphigus showed reactivity with recombinant Dsc 1-3, Dsg 1, and Dsg3 protein (Figure 2B, lower panel).

### Purification of Dsc3-Reactive IgG from Pemphigus Sera

Affinity chromatography columns were prepared with CNBr-activated sepharose 4B (Amersham Biosciences) diluted in 1

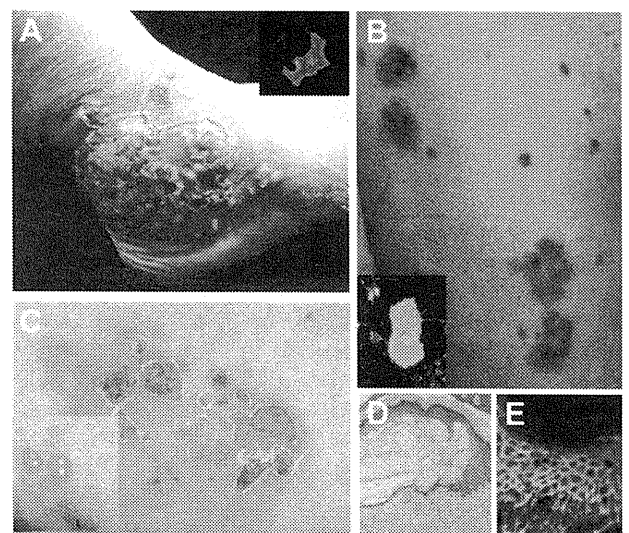


**Figure 1.** Clinical phenotype of representative patients with atypical pemphigus. Clinical pictures of two representative patients with atypical pemphigus (pemphigus vegetans and pemphigus herpetiformis), illustrating hypertrophic verrucous plaques with pustules and erosions of the foot (A) and multiple erythematous herpetiform erosions of the trunk and extremities (B, C). Insets in A and B show IgG reactivity of the patients' sera with human desmocollin 3-transfected COS-7 cells. Histopathology of lesional skin reveals intraepidermal loss of keratinocyte adhesion at the suprabasilar level (D). Direct immunofluorescence shows IgG deposits on the surface of epidermal keratinocytes (E).

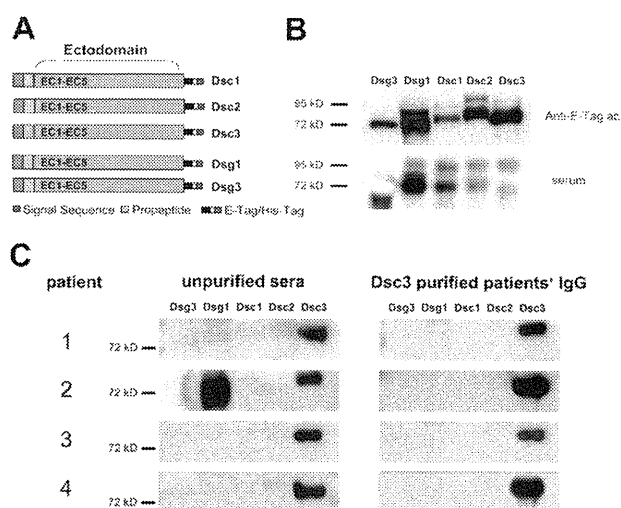


**Figure 2.** Affinity purification of desmocollin 3 (Dsc3)-reactive IgG autoantibodies from four patients with atypical pemphigus. **A:** Scheme of the recombinant proteins applied in this study, ie, the entire ectodomains of Dsc1, Dsc2, Dsc3, desmoglein 1 (Dsg1), and desmoglein 3 (Dsg3) linked to E- and 6xHis-Tag. **B:** Detection of the recombinant proteins by immunoblot analysis using an anti-E-tag monoclonal antibody (**upper panel**) or serum of a patient with paraneoplastic pemphigus (**lower panel**). **C:** Immunoblot analysis revealing IgG reactivity of the four atypical pemphigus sera, with the recombinant proteins before (**left panels**) and after (**right panels**) affinity purification, using Dsc3 columns. Patient 2 shows additional IgG reactivity with Dsg1.

mmol/L HCl as recommended by the manufacturer. Before coupling, the ligands (recombinant Dsc3 or Dsg3) were dialyzed against coupling buffer (0.1 M NaHCO<sub>3</sub>, 0.5 M NaCl, pH 8.3) and incubated with the sepharose medium overnight at 4°C. The next day, the coupled sepharose was subjected to five washes with coupling buffer followed by incubation with blocking buffer (0.1 M Tris-HCl at pH 8.0) for 2 hours at room temperature. The coupled sepharose was then washed four times with 0.1 M acetate and 0.5 M NaCl at pH 4.0 and four times with 0.1 M Tris-HCl and 0.5 M NaCl at pH 8.0 alternately. Finally, the sepharose was washed with PBS containing 0.5 mmol/L CaCl<sub>2</sub> at pH 7.4.

Pemphigus sera were diluted at 1:5 in PBS containing 0.5 mmol/L CaCl<sub>2</sub> at pH 7.4. The Dsc3 column was incubated with the diluted sera overnight at 4°C. The next day, the pre-adsorbed sera were collected and the column was washed three times with PBS containing 0.5 mmol/L CaCl<sub>2</sub> + 0.05% Tween 20 at pH 7.4 and, subsequently, three times with PBS containing 0.5 mmol/L CaCl<sub>2</sub> at pH 7.4. The antibodies were eluted using 100 mmol/L Glycin-HCl (pH 2.7), and 900 μL aliquots were collected in tubes containing 100 μL of 1 M Tris-HCl (pH 9.0). The antibodies containing aliquots were combined (total volume of 15 ml) and dialyzed overnight against PBS with 0.5 mmol/L CaCl<sub>2</sub> at pH 7.4. The purified IgG fraction was concentrated 10-fold using Amicon Ultra-15 Centrifugal Filter Units (Millipore, Billerica, MA). The protein concentration of the eluate was measured using a modified Lowry protein assay. Final protein concentrations ranged between 100 and 200 μg/ml.

### Immunoblot Analysis with Dsc and Dsg Recombinants

The Dsg and Dsc recombinants were run on 10% SDS-PAGE and blotted onto nitrocellulose membranes as previ-

ously described.<sup>9,15</sup> Membranes were blocked with 5% milk powder in PBS, 0.05% Tween-20 (PBS-T) with 0.5 mmol/L CaCl<sub>2</sub>. Pemphigus sera (1:100) and purified IgG fractions (1:20) were diluted in PBS-T with 0.5 mmol/L CaCl<sub>2</sub> and 5% milk powder and were incubated with the blotted membranes overnight at 4°C. After three washes with PBS-T supplemented with 0.5 mmol/L CaCl<sub>2</sub>, the nitrocellulose membranes were incubated with horseradish peroxidase (HRP)-conjugated anti-human IgG (1:5000; Dako, Glostrup, Denmark) for 1 hour at room temperature. Specific immunoreactivity was then visualized using Immobilon Western Chemiluminescent HRP substrate (Millipore) (Figure 2, B and C).

### Immunofluorescence Studies

The immortalized keratinocyte cell line HaCaT was cultured in Dulbecco's modified Eagle's medium (DMEM high glucose; Invitrogen) supplemented with 10% fetal calf serum (PAA, Pasching, Austria), 50 units/ml penicillin-G, 50 μg streptomycin and 2 mmol/L L-Glutamine (Gibco, Karlsruhe, Germany). For immunofluorescence staining, HaCaT cells were grown subconfluent in chamber slides (Nunc/Thermo, Fisher Scientific, Wiesbaden, Germany) using epidermal keratinocyte medium (CnT-57 medium; CELLnTEC Advanced Cell Systems, Bern, Switzerland). Subconfluent keratinocyte cultures were switched to defined keratinocyte medium (CnT-02 medium; CELLnTEC Advanced Cell Systems) supplemented with 1.2 mmol/L CaCl<sub>2</sub> 24 hours before adding the IgG fractions. Keratinocytes were then incubated for 2 hours at 4°C with purified anti-Dsc3 IgG diluted at 1:2, pooled IgG from healthy donors 1:2 diluted or anti-Dsc3 monoclonal antibodies (clone U114, 1 μg/ml; Progen, Heidelberg, Germany). After three washes with PBS containing 1.2 mmol/L CaCl<sub>2</sub> and 1.0 mmol/L MgCl<sub>2</sub> 6H<sub>2</sub>O, keratinocytes were fixed in 1% paraformaldehyde-PBS for 20 minutes at room temperature. After three washes, cells were incubated with PBS containing 0.5% Triton X-100 for 10 minutes at room temperature and were finally incubated with fluorescein isothiocyanate (FITC)-labeled anti-human IgG at 1:200 in 1% bovine serum albumin-PBS (dianova, Hamburg, Germany) (Figure 3A-F).

Frozen sections of normal human skin were blocked for 30 minutes with PBS supplemented with 10% normal goat serum. Samples were incubated for 1 hour at room temperature with purified Dsc3-reactive IgG (diluted in PBS with 2% goat serum at 1:2), IgG pooled from healthy donors at the same dilution or anti-Dsc3 monoclonal IgG (U114; Progen) as positive control for Dsc3 reactivity. After three washes with PBS, the skin sections were incubated with FITC-labeled rabbit anti-human IgG (1:200; dianova) for 30 minutes at room temperature (Figure 3G-L).

Indirect immunofluorescence on monkey esophagus was performed following a standardized protocol according to the manufacturer's instructions (The Binding Site, Birmingham, UK). (Figure 3M-R).

### Dispase-Based Keratinocyte Dissociation Assay

Primary human epidermal keratinocytes were seeded in 12-well plates and grown to confluence in CnT-57 medium



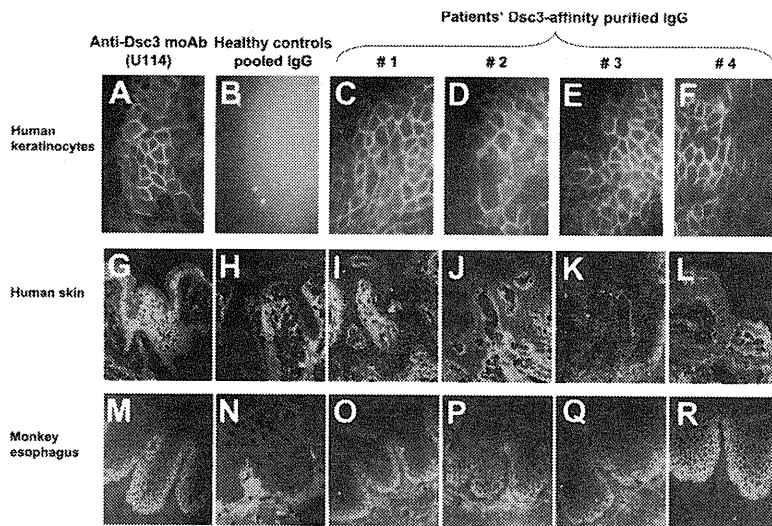


**Figure 3.** Reactivity of the purified desmocollin 3 (Dsc3)-reactive IgG autoantibodies with cultured human keratinocytes, human epidermis, and monkey esophagus. Dsc3 affinity-purified IgG from four patients, with atypical pemphigus, reveal intercellular reactivity with cultured human keratinocytes (HaCaT cells) [patients 1–4 (C–F)], human epidermis (I–L) and monkey esophagus (O–R). Monoclonal anti-Dsc3 antibody (clone U114) (A, G, and M) and pooled IgG of healthy control sera (B, H, and N) served as positive and negative controls, respectively.

(CELLnTEC Advanced Cell Systems) as previously described.<sup>16</sup> The day before the assay, cells were cultured in CnT-02 medium (CELLnTEC Advanced Cell Systems) containing 1.2 mmol/L CaCl<sub>2</sub> and incubated with purified Dsc3-reactive IgG (at 20 µg/ml), pooled control IgG (20 µg/ml) or anti-Dsc3 monoclonal antibody (U114 at 1 µg/ml; Progen), overnight at 37°C. Two hours before the assay termination, recombinant exfoliative toxin A (Toxin Technology, Sarasota, FL) was added at 0.5 µg/ml to cleave Dsg1 on the keratinocyte surface. After two washes with PBS, the adherent keratinocytes were incubated at 37°C for 20 minutes with dispase I (Roche Applied Sciences, Mannheim, Germany) resulting in a non-adherent cell monolayer. The monolayers were carefully washed twice with PBS and subjected to mechanical stress by pipetting ten times with a 1-ml pipet. Fragments were fixed in 1 ml of a 10% formalin solution and stained with crystal violet. Images were captured using a digital camera and fragments were counted

by five different blinded observers (Figure 4). Relative dissociation scores were calculated using the number of keratinocyte fragments in relation to the maximal number of cell fragments obtained by the positive control (anti-dsc3 monoclonal antibody, clone U114).

## Results

### Dsc3-Reactive Autoab in the Sera of Four Patients with Atypical Pemphigus

Sera of four patients with pemphigus herpetiformis and pemphigus vegetans, respectively, were included in this study. Patients presented with multiple erythematous herpetiform erosions and with hypertrophic verrucous plaques with pustules and erosions, respectively, which are illustrated in Figure 1. Histopathology analysis of le-

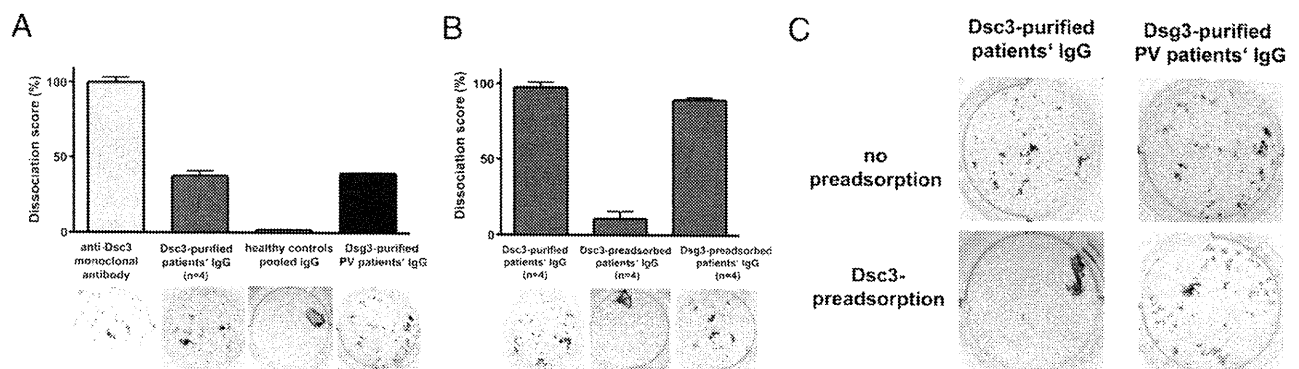


**Figure 4.** Desmocollin 3 (Dsc3)-affinity purified IgG from four patients with atypical pemphigus induces loss of keratinocyte adhesion. Results of the dispase-based keratinocyte dissociation assay using primary human epidermal keratinocytes are illustrated. Keratinocyte monolayers were incubated with the monoclonal anti-Dsc3 IgG antibody (clone U114), Dsc3-affinity purified IgG from the four atypical pemphigus patients, pooled IgG from healthy donors, or desmoglein 3 (Dsg3)-affinity purified IgG from a pemphigus vulgaris patient. **A:** Quantification of the keratinocyte fragments is depicted as a relative dissociation score. The maximal number of keratinocyte fragments obtained after incubation with the monoclonal anti-Dsc3 IgG antibody (clone U114) is set as 100%. Representative images out of three independent experiments are shown below the diagram. **B:** Number of keratinocyte fragments after incubation with Dsc3-affinity purified IgG from four atypical pemphigus patients is illustrated as a dissociation score of 100% (**B, left column**). The induction of keratinocyte dissociation is Dsc3-specific because pre-adsorption of the Dsc3-affinity purified IgG fraction with recombinant Dsc3 (**B, middle column** and **C, left panel**) but not with human Dsg3 (**B, right column**) blocks keratinocyte dissociation. To exclude non-specific binding of IgG to recombinant Dsc3 protein, Dsg3-purified IgG from a pemphigus vulgaris patient was pre-adsorbed with Dsc3 protein (**C, right panels**). Dsg3 affinity purified IgG induces loss of keratinocyte adhesion (**A** and **C**) that is not inhibited by pre-adsorption with human Dsc3 protein (**C, right panels**).

sional skin indicated intraepidermal loss of keratinocyte adhesion at the suprabasilar layer (Figure 1D). Furthermore, direct immunofluorescence revealed an intercellular staining pattern, ie, positive IgG deposits on the surface of epidermal keratinocytes (Figure 1E).

To identify the desmosomal target proteins recognized by the IgG autoab of these patients, the sera were reacted with defined baculovirus-derived proteins including Dsg1, Dsg3, and Dsc1-3<sup>9,15</sup> (Figure 2, A and B, upper panel). Immunoblot analysis revealed the presence of IgG against Dsc3 in all of the studied patients; in addition, the serum of patient 2 showed IgG reactivity against Dsg1 (Figure 2C, left panel; Table 1).

### *Dsc3-Specific IgG Recognizes Recombinant and Native Dsc3*

Serum samples of four atypical pemphigus patients were affinity purified using a Dsc3-coupled-CNBr sepharose column to obtain and further analyze the Dsc3-reactive IgG fraction. After purification, the IgG fractions of the four studied patients reacted exclusively with recombinant Dsc3, which was indicated by immunoblot analysis (Figure 2C, right panels). To determine the reactivity of the Dsc3-purified IgG also with native Dsc3, immunofluorescence of cultured human keratinocytes (HaCat) and human skin samples was also performed (Figure 3). The anti-Dsc3 monoclonal antibody U114 was used as a positive control and showed intercellular staining of both keratinocyte cell surface (Figure 3A) and human epidermis (Figure 3G), whereas pooled IgG from healthy control sera did not show any specific staining (negative control, Figure 3B, H). The Dsc3-purified IgG fractions of patients 1–4 demonstrated intercellular reactivity with cultured human keratinocytes (Figure 3C–F) and human epidermis (Figure 3I–L). In addition, indirect immunofluorescence was performed on monkey esophagus confirming the previous results (Figure 3M–R). The anti-Dsc3 monoclonal antibody, U114, elicited an intercellular staining pattern predominantly at the expected basal and suprabasal levels of the mucosal epithelium (Figure 3M). Very similar results were obtained subjecting the Dsc3-purified IgG fractions of patients 1–4 to immunofluorescent staining on monkey esophagus (Figure 3O–R), demonstrating the binding of these Dsc3-purified autoab to native Dsc3.

### *Dsc3-Specific IgG Induces Loss of Keratinocyte Adhesion in Vitro*

After confirming the reactivity of Dsc3-purified IgG autoab with recombinant and native Dsc3, we sought to investigate the pathogenic relevance of these autoab. Interference with keratinocyte adhesion is considered the pathogenic hallmark of autoab in pemphigus. Thus, we applied a well established *in vitro* system for evaluating the capability of Dsc3-purified IgG autoab to induce loss of keratinocyte adhesion.<sup>16</sup> Dsc3-purified IgG of pemphigus patients 1–4 was applied to a dispase-based keratinocyte dissociation assay using primary human keratinocytes. Confluent grown primary keratinocytes were incubated with Dsc3-

purified IgG fractions of patients 1–4, and afterwards Dsg1 was degraded by incubation with exfoliatin A. Next, mechanical stress was applied to the keratinocyte monolayer to obtain cellular fragments illustrating the loss of keratinocyte adhesion in these keratinocyte cultures and thus, the pathogenicity of the Dsc3 autoab studied. Figure 4 illustrates that the anti-Dsc3 monoclonal antibody, U114, induces a dramatic weakening of keratinocyte adhesion, leading to a high number of keratinocyte fragments, whereas control IgG from pooled healthy individuals does not affect keratinocyte adhesion (Figure 4A). Keratinocyte cell sheets incubated with Dsc3-purified IgG were dissociated into numerous smaller fragments, indicating that Dsc3-reactive IgG of patients' sera is capable of inducing loss of keratinocyte adhesion (Figure 4A).

Furthermore, it was crucial to investigate whether this effect on keratinocyte adhesion was specific for the Dsc3-reactive autoab and related to the presence of Dsc3 in desmosomes. Pre-adsorption of the Dsc3-purified IgG fractions with recombinant Dsc3, but not with recombinant Dsg3, completely blocked the loss of keratinocyte adhesion in the dissociation assay (Figure 4B). To exclude non-specific binding of IgG autoab to recombinant Dsc3, we also applied Dsg3-purified IgG from PV patients to the keratinocyte dissociation assay. As previously described, Dsg3-reactive autoab of a pemphigus vulgaris patient induces loss of keratinocyte adhesion in this assay (Figure 4, A and C). However, pre-incubation of anti-Dsg3 IgG with recombinant Dsc3 protein did not abrogate this effect (Figure 4C, right panel). Thus, these results strongly suggest that the Dsc3-purified IgG fraction in the atypical pemphigus patients studied here is pathogenic and induces loss of keratinocyte adhesion by specifically binding and/or blocking Dsc3 and such effect can be blocked by preincubation with the recombinant Dsc3-protein, but not with Dsg3.

### *Discussion*

This study presents that Dsc3-reactive autoab from patients with atypical pemphigus induce loss of epidermal keratinocyte adhesion. The affinity-purified Dsc3 autoab from the four atypical pemphigus patients induced loss of cellular adhesion in a dispase-based keratinocyte dissociation assay. These results extend recent findings of Spindler et al,<sup>14</sup> which identified Dsc3 as a crucial component of desmosomal adhesion. Moreover, they reported that epidermal adhesion mediated by Dsc3 is inhibited by sera from a subset of patients with atypical pemphigus.<sup>14</sup> IgG autoab against Dsc3 are not exclusively associated with atypical pemphigus; we and others have also identified IgG reactivity against Dsg1 and Dsg3 in single cases of pemphigus herpetiformis.<sup>17,18</sup>

The best evidence that Dsc3 is critically involved in desmosomal adhesion in the epidermis comes from a recently established *Dsc3*<sup>-/-</sup> mouse model.<sup>13</sup> The *Dsc3*<sup>-/-</sup> mice revealed an impressive phenotype with extensive intraepidermal blistering and telogen hair loss. This phenotype shares some similarities with a mouse deficient of Dsg3, the autoantigen of PV.<sup>19</sup> Thus, in addition to Dsg3 and Dsg1,

Dsc3 must be considered as a relevant component for desmosomal adhesion of epidermal keratinocytes.

Until now, there was only circumstantial evidence for a pathogenic role of IgG autoab against distinct Dsc isoforms. Dsc1 has been previously identified as a target antigen of IgA autoab in the subcorneal pustular dermatosis type of IgA pemphigus.<sup>8,20</sup> Except for the findings of a single *in vitro* study,<sup>21</sup> there is currently no clear evidence for the pathogenicity of IgA autoab on desmosomal cell-cell adhesion. Autoab against Dsc of the IgG and IgA classes have been occasionally identified in patients with atypical pemphigus<sup>9,10,12,17</sup> and paraneoplastic pemphigus.<sup>9,22,23</sup>

It is currently a matter of debate whether IgG or IgA autoab against Dsc are rare phenomena in pemphigus or whether their detection is limited by the diagnostic tools that are currently available. Hisamatsu et al<sup>11</sup> did not detect IgG or IgA autoab against Dsc1-3 in 45 sera from classical pemphigus patients by enzyme-linked immunosorbent assay (ELISA) with recombinant proteins. The sensitivity of the Dsc-ELISA was limited because all of the sera from eight patients with IgA pemphigus revealed IgA reactivity with Dsc1 expressed on COS cells, but only one serum was IgA positive by ELISA.<sup>11</sup> Using baculovirus-derived, eukaryotic recombinants of Dsc1, Dsc2, and Dsc3, Müller et al<sup>9</sup> were not able to detect Dsc-specific IgG in the sera of a cohort of 74 European patients with PV by ELISA and immunoblot, respectively. However, a considerable number of sera from patients with atypical forms of pemphigus, paraneoplastic pemphigus, and IgA pemphigus demonstrated either IgG or IgA reactivity with Dsc1, Dsc2, or Dsc3.<sup>9</sup> This observation is also reflected by the findings of the present study that the four Dsc3-reactive sera studied here were derived from patients with atypical pemphigus (pemphigus vegetans and pemphigus herpetiformis) who presented with cutaneous blisters; additional IgG reactivity against Dsg1 was found in only one case. Thus, the low detection rate of Dsc-reactive IgG autoab in PV and PF is presumably not a technical artifact, rather it is due to the low prevalence of Dsc-reactive autoab in PV or PF.

In summary, the present findings demonstrate that IgG autoab against Dsc3 induce loss of keratinocyte adhesion, which strongly suggests their pathogenic relevance in pemphigus. Because Dsc3-reactive IgG is only rarely found in patients with classical PV or PF, the observed *in vitro* pathogenicity of anti-Dsc3 IgG autoab provides a sound explanation why Dsc3-reactive patients with atypical pemphigus lacking IgG against Dsg3 or Dsg1 develop skin blistering.

### Acknowledgments

We are grateful to Eva Podstawa, Nadine Losse, and Andrea Gerber for excellent technical assistance.

### References

1. Amagai M, Klaus-Kovtun V, Stanley JR: Autoantibodies against a novel epithelial cadherin in pemphigus vulgaris, a disease of cell adhesion. *Cell* 1991, 67:869–877
2. Hertl M, Eming R, Veldman C: T cell control in autoimmune bullous skin disorders. *J Clin Invest* 2006, 116:1159–1166

3. Amagai M, Hashimoto T, Shimizu N, Nishikawa T: Absorption of pathogenic autoantibodies by the extracellular domain of pemphigus vulgaris antigen (Dsg3) produced by baculovirus. *J Clin Invest* 1994, 94:59–67
4. Mahoney MG, Wang Z, Rothenberger K, Koch PJ, Amagai M, Stanley JR: Explanations for the clinical and microscopic localization of lesions in pemphigus foliaceus and vulgaris. *J Clin Invest* 1999, 103:461–468
5. Amagai M, Koch PJ, Nishikawa T, Stanley JR: Pemphigus vulgaris antigen (desmoglein 3) is localized in the lower epidermis, the site of blister formation in patients. *J Invest Dermatol* 1996, 106:351–355
6. Green KJ, Simpson CL: Desmosomes: new perspectives on a classic. *J Invest Dermatol* 2007, 127:2499–2515
7. Cheng X, Den Z, Koch PJ: Desmosomal cell adhesion in mammalian development. *Eur J Cell Biol* 2005, 84:215–223
8. Hashimoto T, Kiyokawa C, Mori O, Miyasato M, Chidgey MA, Garrod DR, Kobayashi Y, Komori K, Ishii K, Amagai M, Nishikawa T: Human desmocollin 1 (Dsc1) is an autoantigen for the subcorneal pustular dermatosis type of IgA pemphigus. *J Invest Dermatol* 1997, 109:127–131
9. Müller R, Heber B, Hashimoto T, Messer G, Mullegger R, Niedermeier A, Hertl M: Autoantibodies against desmocollins in European patients with pemphigus. *Clin Exp Dermatol* 2009, 34:898–903
10. Hashimoto T, Amagai M, Watanabe K, Dmochowski M, Chidgey MA, Yue KK, Garrod DR, Nishikawa T: A case of pemphigus vulgaris showing reactivity with pemphigus antigens (Dsg1 and Dsg3) and desmocollins. *J Invest Dermatol* 1995, 104:541–544
11. Hisamatsu Y, Amagai M, Garrod DR, Kanzaki T, Hashimoto T: The detection of IgG and IgA autoantibodies to desmocollins 1-3 by enzyme-linked immunosorbent assays using baculovirus-expressed proteins, in atypical pemphigus but not in typical pemphigus. *Br J Dermatol* 2004, 151:73–83
12. Dmochowski M, Hashimoto T, Chidgey MA, Yue KK, Wilkinson RW, Nishikawa T, Garrod DR: Demonstration of antibodies to bovine desmocollin isoforms in certain pemphigus sera. *Br J Dermatol* 1995, 133:519–525
13. Chen J, Den Z, Koch PJ: Loss of desmocollin 3 in mice leads to epidermal blistering. *J Cell Sci* 2008, 121:2844–2849
14. Spindler V, Heupel WM, Efthymiadis A, Schmidt E, Eming R, Rankl C, Hinterdorfer P, Müller T, Drenckhahn D, Waschke J: Desmocollin 3-mediated binding is crucial for keratinocyte cohesion and is impaired in pemphigus. *J Biol Chem* 2009, 284:30556–30564
15. Müller R, Svoboda V, Wenzel E, Müller HH, Hertl M: IgG against extracellular subdomains of desmoglein 3 relates to clinical phenotype of pemphigus vulgaris. *Exp Dermatol* 2008, 17:35–43
16. Ishii K, Harada R, Matsuo I, Shirakata Y, Hashimoto K, Amagai M: *In vitro* keratinocyte dissociation assay for evaluation of the pathogenicity of anti-desmoglein 3 IgG autoantibodies in pemphigus vulgaris. *J Invest Dermatol* 2005, 124:939–946
17. Kozłowska A, Hashimoto T, Jarzabek-Chorzelska M, Amagai A, Nagata Y, Strasz Z, Jablonska S: Pemphigus herpetiformis with IgA and IgG antibodies to desmoglein 1 and IgG antibodies to desmocollin 3. *J Am Acad Dermatol* 2003, 48:117–122
18. Lebeau S, Müller R, Masouyé I, Hertl M, Borradori L: Pemphigus herpetiformis: analysis of the autoantibody profile during the disease course with changes in the clinical phenotype. *Clin Exp Dermatol* 2010, 35:366–372
19. Koch PJ, Mahoney MG, Ishikawa H, Pulkkinen L, Uitto J, Shultz L, Murphy GF, Whitaker-Menezes D, Stanley JR: Targeted disruption of the pemphigus vulgaris antigen (desmoglein 3) gene in mice causes loss of keratinocyte cell adhesion with a phenotype similar to pemphigus vulgaris. *J Cell Biol* 1997, 137:1091–1102
20. Heng A, Nwaneshiudu A, Hashimoto T, Amagai M, Stanley JR: Intraepidermal neutrophilic IgA/IgG antidesmocollin 1 pemphigus. *Br J Dermatol* 2006, 154:1018–1020
21. Supapannachart N, Mutasim DF: The distribution of IgA pemphigus antigen in human skin and the role of IgA anti-cell surface antibodies in the induction of intraepidermal acantholysis. *Arch Dermatol* 1993, 129:605–608
22. Chorzelski TP, Hashimoto T, Nishikawa T, Ebihara T, Dmochowski M, Ismail M, Jablonska S: Unusual acantholytic bullous dermatosis associated with neoplasia and IgG and IgA antibodies against bovine desmocollins I and II. *J Am Acad Dermatol* 1994, 31:351–355
23. Hashimoto T: Immunopathology of paraneoplastic pemphigus. *Clin Dermatol* 2001, 19:675–682

management in cutaneous melanoma. In up to 5% of patients, cutaneous metastases can even be the first manifestation of the disease [1]. In many cases, cutaneous metastases present as painless, firm, blue or red coloured subcutaneous nodules, but some metastases may adopt unusual appearances, simulating other benign or malignant conditions that may cause difficulties for diagnosis [2, 3]. We here present a case of a cutaneous melanoma metastasis mimicking a pyogenic granuloma.

Pyogenic granuloma is a common benign skin tumour that usually presents as a solitary, rapidly growing papule that bleeds easily after minor trauma. Not uncommonly, dermatologists or family doctors might be the first physicians faced with this type of skin lesion, which is especially frequent in children and younger adults. The etiology of pyogenic granuloma is unknown, but prior skin trauma, chronic irritation, infection (e.g. with *Bartonella* species) as well as the influence of estrogens and other steroid hormones are cited as predisposing factors [4]. Clinically, the differential diagnoses include vascular tumours like Kaposi sarcoma, hemangi endothelioma, angiosarcoma as well as bacillary angiomatosis, but also other skin neoplasms, e.g. amelanotic melanoma, squamous cell carcinoma, basal cell carcinoma and cutaneous metastasis have to be considered. The most important features favouring the clinical diagnosis of pyogenic granuloma are its rapid enlargement (in the range of a few weeks) and its tendency to bleed easily. Angio-mode Doppler sonography typically depicts one or several vessels with branching within an exophytic echopoor tumour [5]. However, although all of these clinical and ultrasound criteria were positive in our patient, the histopathologic examination of the excised tumour figured out the diagnosis of a cutaneous melanoma metastasis. The case presented herein illustrates the necessity of microscopic examination of presumed pyogenic granuloma, especially in patients with a previous malignant disease. ■

**Disclosure.** Financial support: none. Conflict of interest: none.

<sup>1</sup> Department of Dermatology and Allergology, Center of Integrated Oncology (CIO) Cologne Bonn, University of Bonn, Sigmund-Freud-Str. 25, D-53127 Bonn, Germany  
<sup>2</sup> Department I of Internal Medicine, CIO Cologne Bonn, University of Cologne, Cologne, Germany  
 <Monika-Hildegard.Schmid-Wendtner@ukb.uni-bonn.de>

Torsten HINZ<sup>1</sup>  
 Joerg WENZEL<sup>1</sup>  
 Clemens-M. WENDTNER<sup>2</sup>  
 Monica-H. SCHMID-WENDTNER<sup>1</sup>

1. Plaza JA, Torres-Cabala C, Evans H, *et al.* Cutaneous metastases of malignant melanoma: a clinopathologic study of 192 cases with emphasis on the morphologic spectrum. *Am J Dermatopathol* 2010; 32: 129-36.
2. Egberts F, Kaehler KC, Brasch J, *et al.* Multiple skin metastases of malignant melanoma with unusual clinical and histopathologic features in an immunosuppressed patient. *J Am Acad Dermatol* 2008; 58: 880-4.

3. Hussein MRA. Skin metastasis: a pathologist's perspective. *J Cutan Pathol* 2010; 37: e1-e20.
4. Levy I, Rolain JM, Lepidi H, *et al.* Is pyogenic granuloma associated with *Bartonella* infection?. *J Am Acad Dermatol* 2005; 53: 1065-6.
5. Wortsman X, Wortsman J. Clinical usefulness of variable-frequency ultrasound in localized lesions of the skin. *J Am Acad Dermatol* 2010; 62: 247-56.

doi:10.1684/ejd.2010.1181

## Paraneoplastic pemphigus associated with non-Hodgkin's lymphoma

Paraneoplastic pemphigus (PNP) is an autoimmune blistering disease described first by Anhalt *et al.* in 1990 [1]. PNP is mainly associated with hematological proliferative disorders [1]. Among them, non-Hodgkin's lymphoma (NHL) is most commonly associated. Recently, rituximab, an anti-CD20 monoclonal antibody, has been used for the treatment of NHL and PNP [2, 3]. Here, we describe a 57-year-old female patient with PNP associated with follicular, CD20-positive NHL, treated with a regime including rituximab. A 57-year-old Japanese woman visited the Division of Internal medicine with a 2-week history of general fatigue, malaise, and loss of weight, in January 2005. She was diagnosed as having NHL (follicular, CD20-positive, stage IV) in April 2005, and received 6 courses of cyclophosphamide, doxorubicin, vincristine and prednisolone plus rituximab (R-CHOP). The clinical response was evaluated

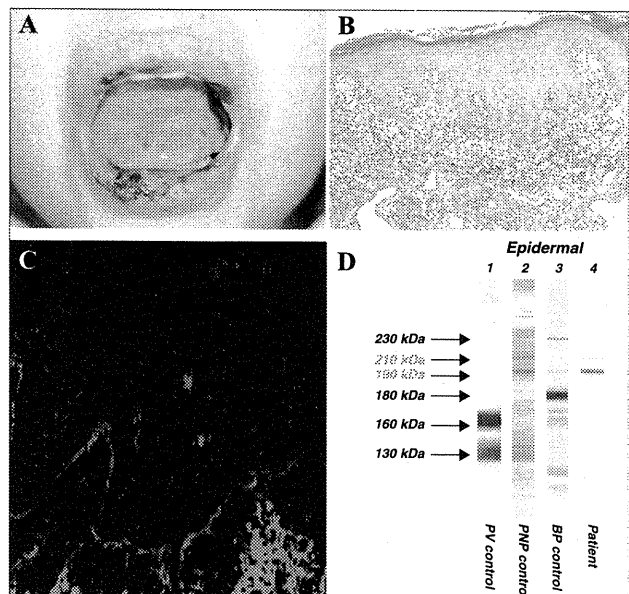


**Figure 1.** A) Numerous ulcers on the lips, and the tongue. B) Histopathological examination (HE stain). C) Direct immunofluorescence exhibited IgG deposition at both the cell surfaces and the basement membrane zone in the epidermis. D) Immunoblot analysis using normal human epidermal extracts.

**Table 1.** Summary of cases of PNP treated with rituximab.

Case	Age (years)/gender	Diagnosis	Treatment prior to rituximab	Outcome
1	73/F	CD20-positive follicular NHL	PSL, cyclophosphamide	Clearance of conjunctiva and mucocutaneous lesions after 6 months of rituximab, and partial remission of NHL
2	61/F	CD20-positive follicular NHL	Cyclophosphamide, doxorubicin, vincristine, PSL	Clearance of mucosal lesions after 2 months of rituximab and partial tumor regression
3	79/F	Gastric B-cell lymphoma of MALT type	Radiotherapy, PSL, mycophenolate mofetil	Clearance of skin and oral mucosal lesions after 2 months of rituximab. Died suddenly during rehabilitation, no autopsy performed
4	70/M	CD20-positive follicular NHL	1998: chlorambucil, cyclophosphamide, vincristine, PSL, fludarabine, local radiotherapy 2002: PSL, dexamethasone, azathioprine	2002: after 8 weeks of rituximab, slight response in cutaneous lesions and NHL, but mucosal lesions responded poorly. Died of cardiac failure and pulmonary edema
5	64/F	Small B-cell lymphoma; Waldenstrom's macroglobulinemia	Fludarabine (1 year prior to rituximab) Sulfasalazine, PSL, cyclophosphamide	Underwent 2 weeks of rituximab with no improvement of mucocutaneous lesions. Died of sepsis shortly after
6	49/F	CD20-positive follicular NHL	1999: CHOP, radiotherapy, fludarabine, mitozantrone, dexamethasone 2003: fludarabine 2005: cyclophosphamide, vincristine, PSL	2005: initial improvement in mucocutaneous lesions and NHL after 4 weeks of rituximab. Recurrence of mucocutaneous lesions, died after 8 weeks of rituximab
7	77/F	CD20-positive follicular NHL	PSL, cyclosporine	2001: oral ulcerations improved and NHL showed a 25% decrease of lymph nodes after 4 weeks of rituximab

MALT: mucosa-associated lymphoid tissue, PSL: prednisolone, CHOP: cyclophosphamide, doxorubicin, vincristine and PSL.

References of cases. 1: [2], 2: [3], 3: Ahmad AR, et al. *N Engl J Med* 2003; 349: 382-91, 4: Rossum MM, et al. *Leukaemia Lymphoma* 2004; 45: 2327-32, 5: Schadlow MB, et al. *J Drugs Dermatol* 2003; 2: 564-7, 6: Hoque SR, et al. *Clin Exp Dermatol* 2007; 32: 172-5, 7: Barnadas MA, et al. *J Eur Acad Dermatol Venereol* 2006; 20: 69-74.

as stable. She was referred to our hospital with a 4-month history of painful ulcers in the oral mucosa in December 2007. There were multiple erosions and ulcers on the oral mucosa, lips, and dorsum of the tongue (*figure 1A*). Histopathological examination of a perilesional area on the lip showed vacuolar interface changes with band-like lymphocytic infiltration in the upper dermis (*figure 1B*). Direct immunofluorescence showed IgG deposition at both the cell surfaces and the basement membrane zone in the epidermis (*figure 1C*). Her serum was positive for anti-Dsg3 antibodies, and was negative for anti-Dsg1 antibodies by ELISA. Indirect immunofluorescence showed IgG antibodies binding to rat bladder epithelium, and her serum reacted with the 210 kDa envoplakin and 190 kDa periplakin by immunoblotting, using normal human epidermal extracts (*figure 1D*). We diagnosed this case as PNP, and started oral prednisolone at 50 mg/day, which resulted in the partial improvement of oral erosive lesions within two weeks. She transferred to the previous hospital for NHL treatment, because of enlargement of the lymph nodes detected by PET/CT in January 2008. Despite the therapy of cyclophosphamide, therarubicin, vincristine, prednisolone and rituximab (R-THP-COP), the oral lesions recurred gradually and she died of sepsis during the third course of R-THP-COP in May 2008. No clear effect of R-THP-COP on either NHL or PNP was observed.

Rituximab, a chimeric monoclonal anti-CD20 antibody, was initially approved for relapsed or refractory, low grade or follicular, CD20-positive NHL in the USA in 1997 [4]. The overall response rate was 48%, with 6% of patients showing complete remission. Rituximab may be also effective for both NHL and PNP, as previously reported [2, 3]. To the best of our knowledge, 7 cases of PNP associated with B-cell lymphoma have been treated by rituximab, to date (*table 1*). Similar to our case, no clear response to rituximab was shown in 3 cases (cases 4, 5, and 6). On the other hand, the administration of rituximab combined with prednisolone was effective for mucocutaneous lesions in 4 cases (cases 1, 2, 3, and 6). The period between the initiation of rituximab and recovery of mucocutaneous lesions was 6, 2, 2, and 21 months in these four cases, respectively. Since almost all patients with NHL and PNP succumb within three months to two years after diagnosis, except for a couple of individual reports of long-time survivors by classical immunosuppressive treatments [5], the regime including rituximab may be more effective for PNP than the classical treatments. In addition to the depletion of B cells, several immunological effects for T cells, T-regulatory cells, NK cells, and macrophages by rituximab [6] might be associated with the recovery of PNP. We need to conduct further investigations to identify factors relevant to the response of PNP to rituximab. ■



**Disclosure.** Financial support: none. Conflict of interest: none.

<sup>1</sup> Department of Dermatology, University of Tokushima Institute of Health Biosciences, 3-18-15 Kuramoto-cho, 770-8503 Tokushima-city, Japan  
<sup>2</sup> Department of Dermatology, Kurume University School of Medicine, Fukuoka, Japan  
<ykubo@clin.med.tokushima-u.ac.jp>

Takeshi ISHIGAMI<sup>1</sup>  
Yoshiaki KUBO<sup>1</sup>  
Yoshihiro MATSUDATE<sup>1</sup>  
Shinichi ANSAI<sup>1</sup>  
Seiji ARASE<sup>1</sup>  
Bungo OHYAMA<sup>2</sup>  
Takashi HASHIMOTO<sup>2</sup>

1. Anhalt GJ, Kim SC, Stanley JR, *et al.* Paraneoplastic pemphigus. An autoimmune mucocutaneous disease associated with neoplasia. *N Engl J Med* 1990; 323: 1729-35.
2. Heizmann M, Itin P, Wernli M, *et al.* Successful treatment of paraneoplastic pemphigus in follicular NHL with rituximab: report of a case and review of treatment for paraneoplastic pemphigus in NHL and CLL. *Am J Hematol* 2001; 66: 142-4.
3. Borradori L, Lombardi T, Samson J, *et al.* Anti-CD20 monoclonal antibody (rituximab) for refractory erosive stomatitis secondary to CD20(+) follicular lymphoma-associated paraneoplastic pemphigus. *Arch Dermatol* 2001; 137: 269-72.
4. McLaughlin P, Grillo-López AJ, Link BK. Rituximab chimeric anti-CD20 monoclonal antibody therapy for relapsed indolent lymphoma: half of patients respond to a four-dose treatment program. *J Clin Oncol* 1998; 16: 2825-33.
5. Anhalt GJ. Paraneoplastic pemphigus. *J Invest Dermatol Symp Proc* 2004; 9: 29-33.
6. Kessel A, Rosner I, Toubi E. Rituximab: beyond simple B cell depletion. *Clin Rev Allergy Immunol* 2008; 34: 74-9.

doi:10.1684/ejd.2010.1182

## Oral erosive lichen planus and alopecia areata with Good's syndrome (thymoma with hypogammaglobulinemia)

In May 2007, a 71-year-old female was referred to our department from the odontology unit in our hospital for recurrent erosive and hyperkeratotic lesions of the lip, oral mucosa and tongue that had lasted a year (*figure 1A*). There was no other cutaneous or onychial lesion. Her past history revealed no remarkable disease except for hypertension, treated by candesartan cliexetil since 2004. A biopsy of the lip lesion showed saw-tooth-like acanthosis and lichenoid infiltration of lymphocytes (*figure 1B*), compatible with the features of lichen planus. Direct immunofluorescence study showed no deposit of immunoglobulin or complement (data not shown). In spite of therapies with topical steroids, retinoids, antibiotics and antifungal agents, symptoms did not significantly improve. Skin patch tests for metal allergy were all negative. Serological markers for hepatitis B and C viruses were negative. However, levels of serum gammaglobulin were below normal ranges (IgG 639 mg/dL, IgA 16 mg/dL, IgM 29 mg/dL; normal 870-1700 mg/dL, 110-410 mg/dL, 35-220 mg/dL, respectively).

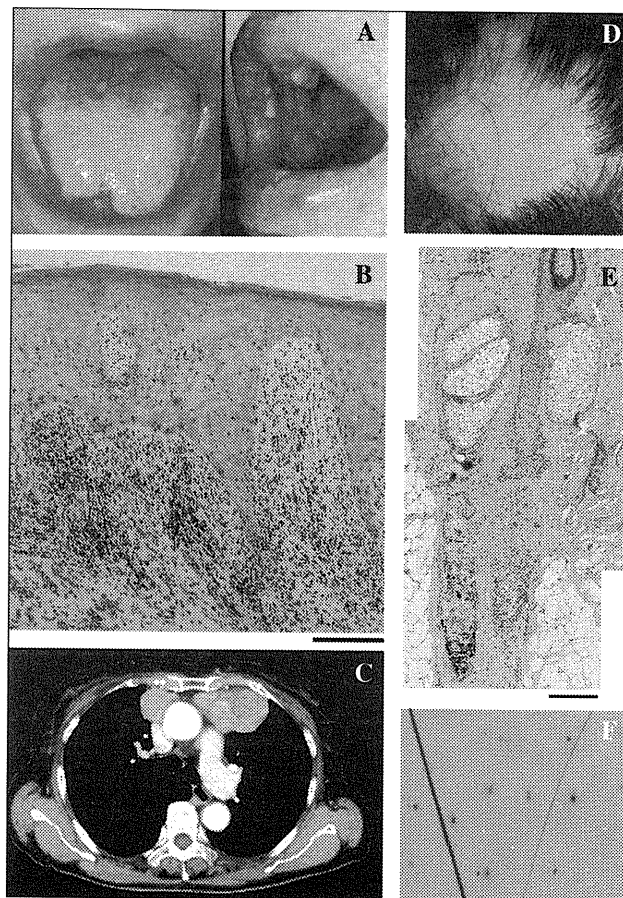


**Figure 1.** A) Multiple erosions with hyperkeratosis on oral mucosa and lips. Erosion of the tongue covered with white fibrous material. B) Histological picture of the lip lesion, consisting of band-like infiltration of lymphocytes in the upper dermis, saw-tooth acanthosis and dyskeratosis (H&E, Bar; 200 micrometer). C) Chest computed tomography showing bilateral masses at the anterior mediastinum. D) Loss of hair on the top of scalp. E) Histological picture of the scalp lesion, consisting of perifollicular infiltration of lymphocytes, loss of hair shaft and dystrophy of hair follicle (H&E, Bar; 200 micrometer). F) Trichoscopic picture of the alopecia, consisting of yellow macules and black dots at the hair follicles.

Computed tomography revealed bilateral thymoma at the anterior mediastinum (*figure 1C*) and a diagnosis of Good's syndrome was made. In April 2009, total thymectomy was performed. Histopathological examination showed type A in the left thymoma and type AB in the right one (according to the WHO classification), and microscopic capsular invasions were seen in both sides. In January 2010, neither hypogammaglobulinemia nor oral erosive lichen planus had disappeared. An abnormality of lymphocyte subpopulation was shown by flow cytometry in February 2010 (CD19 0.0% (normal 6-21%), CD4 24.8% (normal 27-56%) and CD8 47.8% (normal 14-44%) (CD4/CD8 0.5 (normal 0.6-2.8)). In May 2010, non-scarring alopecia developed on the top of the scalp (*figure 1D*). Skin biopsy showed perifollicular infiltration of lymphocytes, loss of hair shafts and dystrophy of hair bulbs (*figure 1E*), but no interface change of hair follicles. Trichoscopic examination showed yellow macules and black dots (*figure 1F*). Taken together, diag-

# Neural System Antigens Are Recognized by Autoantibodies from Patients Affected by a New Variant of Endemic Pemphigus Foliaceus in Colombia

Ana Maria Abreu-Velez · Michael S. Howard ·  
Hong Yi · Weiqing Gao · Takashi Hashimoto ·  
Hans E. Grossniklaus

Received: 9 November 2010 / Accepted: 6 December 2010 / Published online: 6 January 2011  
© Springer Science+Business Media, LLC 2010

## Abstract

**Background** Endemic pemphigus foliaceus (EPF), is also known as “fogo selvagem” or “wild fire,” reflecting the intense burning sensation of the skin reported by patients with this disease. Based on this finding, we tested for neural autoreactivity in patients affected by a new variant of EPF (El Bagre-EPF).

**Methods** We tested 20 El Bagre-EPF patients, 20 normal controls from the endemic area, and 20 age- and sex-matched normal controls from outside the endemic area. We tested for autoreactivity to several immunoglobulins and complement. Both human skin and bovine tail were used as antigens.

**Results** We detected autoreactivity to neural structures, mechanoreceptors, nerves, perineural cell layers of the arachnoid envelope around the optic nerve, brain structures, and to neuromuscular spindles; these structures colocalized

with several neural markers. The patient antibodies also colocalized with desmoplakins 1 and 2, with the armadillo repeat protein deleted in velo-cardio-facial syndrome and with p0071 antibodies. Autoreactivity was also found associated with neurovascular bundles innervating the skin, and immunoelectron microscopy using protein A gold against patient antibodies was positive against the nerve axons. Paucicellularity of the intraepidermal nerve endings and defragmentation of the neural plexus were seen in 70% of the cases and not in the controls from the endemic area ( $p < 0.005$ ). Neuropsychological and/or behavioral symptoms were detected in individuals from the endemic area, including sensorimotor axonal neuropathy.

**Conclusions** Our findings may explain for the first time the “pose of pemphigus,” representing a dorsiflexural posture seen in EPF patients vis-a-vis the weakness of the extensor nerves, and furthermore, the autoreactivity to nerves in EPF could explain the “burning sensation” encountered in EPF disease.

A. M. Abreu-Velez (✉) · M. S. Howard  
Georgia Dermatopathology Associates,  
1534 North Decatur Rd. NE, Suite 206,  
Atlanta, GA 30307-1000, USA  
e-mail: abreuvelez@yahoo.com

H. Yi  
Robert P. Apkarian Integrated Electron Microscopy Core,  
Emory University Medical Center,  
Atlanta, GA, USA

W. Gao · H. E. Grossniklaus  
Department of Ophthalmology, Emory University Medical Center,  
Atlanta, GA, USA

T. Hashimoto  
Department of Dermatology, School of Medicine,  
Kurume University,  
Kurume, Japan

**Keywords** Autoantibodies · mechanoreceptor · pacinian corpuscle · nerves · endemic pemphigus foliaceus · epidermal nerve fiber density · myelin basic protein · glial fibrillary acidic protein · CD57 · protein gene product 9.5 · desmoplakins · optic nerve · arachnoid envelope antibodies

## Abbreviations

EPF	Endemic pemphigus foliaceus
El Bagre-EPF	endemic pemphigus foliaceus in El Bagre, Colombia
FS	fogo selvagem
ICS	intercellular stain between the keratinocytes
BMZ	basement membrane zone
DIF and IIF	direct and indirect immunofluorescence

ENFD	epidermal nerve fiber density
SDI	silver diamine ion stain
BP	bullous pemphigoid
MBS	modified Bielschowsky stain
NHP	Nottingham Health Profile
LKS	Lysholm Knee Scale
NDIC	Normarski differential interference contrast confocal microscopy
IHC	immunohistochemistry
CFM	confocal microscopy
IB	immunoblotting
IEM	immunolectron microscopy
ARVCF	armadillo repeat protein deleted in velo-cardio-facial syndrome

## Introduction

We have identified a new variant of EPF in El Bagre, Colombia, S.A. (El Bagre-EPF) [1–8]. Our studies established that this focus exhibits alike features to those described in Senear–Usher syndrome, a disease with combined features of lupus erythematosus and pemphigus [1–8]. This new variant of El Bagre-EPF differs from classic endemic pemphigus foliaceus (EPF) in aspects such as the following: (1) no clinical involvement of children or persons under the age of 30 years occurs, contrary to fogo selvagem (FS) that primarily affects children and young adults, with the highest incidence at 10–30 years of age, and both sexes equally affected; (2) El Bagre-EPF affects predominantly 40- to 60-year-old men, as well as a few post-menopausal women, in contradistinction to EPF; and (3) the main autoantigens are plakins (desmoplakins, envoplakin, periplakin, and plakoglobin), in comparison to EPF, where most autoantigens are desmogleins1 [1–8]. Both EPF as well as in El Bagre-EPF patients have intercellular deposits of immunoglobulins and/or complement showing intercellular stain (ICS) between the keratinocytes, but contrary to El Bagre-EPF, EPF does not exhibit deposits of antibodies and complement at the basement membrane zone (BMZ) of the skin [1–12].

EPF is also known by the name “fogo selvagem” or “wild fire” because patients affected by this illness classically report a burning sensation on the skin [1–12]. Two main questions about EPF remain unknown over almost a century: what explains the burning sensation of the patients’ skin, which represents the hallmark symptom of this disease, and what explains the muscular weakness and the “pose of pemphigus” (a dorsiflexural position of the body), present in most chronically affected patients before the steroid era [1–12].

The population in El Bagre is exposed to tropical diseases, as well as to mercury and other pollutants as a result of gold mining and agricultural chores [3]. We reported the presence of mercury in skin biopsies from people living in the endemic area [3]. Given the burning sensation present in El Bagre-EPF and FS patients and noting that mercury is a neurotoxin, we searched for nerve alterations by hematoxylin and eosin (H&E), silver diamine ion (SDI), and modified Bielschowsky (MBS) staining. We performed direct and indirect immunofluorescence (DIF and IIF), immunohistochemistry (IHC), confocal microscopy (CFM), immunoblotting (IB), and immunolectron microscopy (IEM) to study patient autoreactivity to several neural components.

## Materials and Methods

We examined 20 El Bagre-EPF patients, 20 normal controls from the endemic area, and 20 normal controls from outside of the endemic area (all matched by age, sex, and work activity). In addition, we tested five patient samples of people suffering FS. El Bagre-EPF disease was characterized by epidemiological, immunological, histopathological, and clinical criteria reported elsewhere [1–3]. Simultaneously, we tested for neuropsychological, behavioral, and kinesiological alterations in the subjects of the study (all tested negative for *Mycobacterium leprae*). All cases displayed IgG4 intercellular staining between keratinocytes [1–3]. Sera of the cases were reactive to desmoglein 1 (Dsg1) by IB, by immunoprecipitation, and by enzyme-linked immunosorbent assay [1–3, 8]. In addition, in IB of the El Bagre-EPF, most sera reacted with plakins [including desmoplakins 1 and 2 (DPI and DPII), envoplakin, periplakin, plakoglobin], to bullous pemphigoid (BP) antigens 1 and 2 and to other undetermined molecules [8]. For IIF, we used as substrates human chest skin, rat, mouse, and chipmunk nerve and brain tissue, and monkey esophagus (Oregon Primate Research Center, Portland, Oregon, USA). Selected samples for DIF and IIF were partially fixed in 3% paraformaldehyde [9, 10]. All samples were tested anonymously to comply with institutional review board requirements.

*DIF and IIF* Slides were incubated with the sera at 1:20–1:40 dilutions in phosphate-buffered saline (PBS), rinsed, and then incubated with secondary antibodies [including Fluorescein isothiocyanate (FITC)-conjugated goat anti-human IgG, IgM, IgA, IgD, IgE, C1q, C3c, C3d, albumin, and fibrinogen (all from Dako, Carpinteria, CA, USA)]. We also utilized anti-human total IgG/IgM/IgA antiserum (Zymed®; Invitrogen, Carlsbad, CA, USA) and rhodamine-conjugated goat anti-human IgA/IgM/IgG anti-



serum (Rockland Labs, Rockland, ME, USA). Neural marker colocalization was studied by utilizing anti-human S-100 antibody (Dako), mouse anti-human neuron specific enolase (NSE) (Dako), and Cy3 conjugated anti-glial fibrillary acidic protein (GFAP), (Sigma Aldrich, St. Louis, MO, USA). In addition, we used a multi-epitope cocktail containing anti-desmoplakin I and II (DPI and DPII), anti-armadillo repeat protein deleted in velo-cardio-facial syndrome (anti-ARVCF) and anti-p0071 antibodies (all from Progen). The secondary antibodies were conjugated with Texas Red and/or with Alexa 555 (both from Invitrogen). All sections were then examined with a Nikon Eclipse 50i microscope (Japan). All slides were counterstained with Dapi (Pierce, Rockford, IL, USA) or TO-PRO®-3/DNA (Invitrogen).

**IHC** Immunohistochemistry was used to study the colocalization of patient's autoantibodies with nerves, employing a dual endogenous peroxidase blockage, with the addition of an Envision dual link (Dako). We tested for anti-human IgG, IgM, IgA, IgD, IgE, C1q, C3c, C3d, albumin, and fibrinogen (all from Dako). We also utilized anti-S-100 proteins, GFAP, NSE, and rabbit anti-human myelin basic protein (MBP), anti-neurofilament, CD57, and protein gene product 9.5 (PPG 9.5) (all from Dako).

**SDI and Modified MBS** Samples were prepared as previously described [9], and all biopsies were taken from the chest area for accurate morphometric correlation [9–14]. Nerve density was determined by the average number of positive silver staining fibers in five low power fields under a light microscope [9, 10]. We quantified both the epidermal nerve fiber density (ENFD) and myelinated nerve endings per square millimeter [9–14].

**Autoreactivity to Optic Nerve and Brain Structures** To define autoreactivity of the El Bagre-EPF patients, we assessed immunoreactivity utilizing optic nerve and brain from rat, mouse, and chipmunk sources, and we performed colocalization with DPI, DPII, ARVCF, and p0071 antibodies.

**Colocalization of El Bagre-EPF Autoantibodies and Neural Markers Utilizing CFM** We performed CFM examinations using standard  $\times 20$  and  $\times 40$  objective lenses; each photo-frame included an area of approximately  $440 \times 330 \mu\text{m}$ . Images were obtained using EZ 1 image analysis software (Nikon, Japan).

**Immunoblotting** IB testing for reactivity of IgM and IgG antibodies to bovine tail nerve was performed. The samples were extracted with 0.6 M Tris-HCl, pH 6.8, containing 2% sodium dodecyl sulfate (SDS), 5%  $\beta$ -mercaptoethanol, and 1 mM EDTA, with 1 mM dithiothreitol and protease inhibitors. Extracts were run on a 10% SDS gel. The

proteins were transferred to nitrocellulose membranes, and the immune reactions were carried out with patient and control sera. Chemiluminescence detection performed using an ECL kit including SuperSignal® West Pico Substrate ECL™ (Pierce, Rockford, IL, USA).

**Neurological, Neuropsychological, Behavioral, and Kinesiological Testing** Clinical studies were performed to identify neurological alterations, including autonomic neuropathies [15–17]. Numbness, paresthesias, urinary incontinence, sensitivity to pressure, cold, heat and pain, bedside orthostatic hypotension, a Valsalva ratio, beat-to-beat blood pressure, pupillary responses, and cranial nerves II–XII were assessed.

**Kinesiology Evaluation** We tested for kinesiological movement and skin shriveling in response to immersing the hand in hot or cold water and also utilized the Nottingham Health Profile (NHP) for the evaluation of muscular imbalance or derangement [11–17]. We used the Lysholm Knee Scale (LKS) to study limp support, impaired stair climbing, squatting, walking, running, jumping, atrophy of the thigh, pain, and swelling [16, 17]. All these parameters were rated as none, very mild, moderate, or severe.

**ENFD, Nerve Morphometry, and Histomorphometric Analysis** SDI, MBS, and IHC stains were used on the skin biopsies to quantify the density of intraepidermal axons, as well as the ENFD [12–15].

**Immunoelectron Microscopy** Postembedding immunogold labeling was performed on samples of El Bagre-EPF sera and controls. Peripheral rat nerve was used as an antigen; the tissue was dissected, fixed in 4% glutaraldehyde with 0.2% paraformaldehyde, and embedded in lowicryl® resin. The tissue was then sectioned at 70 nm thickness. The samples were blocked with a solution from Aurion™, Electron Microcopy Sciences (EMS, Hatfield, PA, USA). The grids were then washed with PBS-BSAC (Aurion™, EMS). The primary antibodies were incubated overnight at 4°C. The next day the grids were washed, and a secondary antibody solution, 10 nm gold-conjugated protein A PBS-BSAC (Aurion, EMS™) was applied. The samples were double-stained with uranyl acetate and lead citrate. The samples were observed under a Hitachi H7500 transmission electron microscope. Immunogold particles displaying any pattern of positivity were converted to TIF format.

**Mercury Detection in Hair and Nails** We measured mercury in the hair in all of the cases and controls. After hair washing, 25 mg of hair and/or nails was cut and degreased with acetone. Hair and nail samples were packed separately in ash-free paper and analyzed separately.

Samples were measured following methods described elsewhere [3]. Mercury was measured in an atomic absorption spectrophotometer (MAS 50). The World Health Organization defines a permissible level of mercury in hair of 7 ppm. We scale the results as negative (-) >7 ppm, weak positive >7–14 ppm (+), positive >14–28 ppm (++), very positive from 28 to 56 ppm (strong positive) (+++), and super strong (>56–144 ppm and upper) (++++).

**Statistical Methods** ENFD and myelinated nerve endings per square millimeter were statistically analyzed using the nonparametric Spearman's rank correlation, specifically with a  $p$  value of 0.05 and a single-tailed analysis. We determined that our data followed a normal distribution using the Kolmogorov–Smirnov test and used Student's  $t$  test to evaluate differences in morphology.

## Results

All El Bagre-EPF patients and the five FS patients have a skin burning sensation, and no control from the endemic or non endemic area has this symptom ( $p>0.005$ ).

**Nerve Paucicellularity (Free Ending and Thin Skin Myelinated Nerves) Was Found in Most El Bagre-EPF Patients** We detected reduced ENFD and decrease myelinated nerve fiber density in 70% ( $p>0.005$ ) of the El Bagre-EPF patients and in three of five FS patients by the H&E, IHC, SDI, and MBS stains. We noted damage to subepidermal neural plexus areas in the El Bagre-EPF patients and in three of five FS patients, featuring fragmentation of both myelinated and non-myelinated fibers as well as reduction of the innervations of skin appendices. These findings were noted in only 6% of the control patients from the endemic area and in none normal controls from outside the endemic area. When utilizing antibodies to PPG9.5, CD57, neurofilament, GFAP, NSE, S-100, and MBP, fragmentation of the subepidermal nerve plexus fibers was appreciated, and specific loss of nerve fibers ascending vertically into the epidermis was observed (Figs. 1, 2, 3, 4, and 5).

**Autoreactivity to Neural Structures Colocalizing with Neural Markers** We found autoreactivity to Pacinian corpuscles (PC), mechanoreceptors, nerves, neuromuscular spindles, and neurovascular packages in 70% of El Bagre-EPF and in three of five FS patients ( $p<0.005$ ). No controls show this reactivity. We demonstrated colocalization of the autoreactivity with multiple neural markers, such CD57, neurofilament, PPG 9.5, CD57, neurofilament, PPG 9.5, GFAP, S-100, and MBP (Figs. 1, 2, 3, 4, and 5).

**Autoreactivity to Optic Nerve and Brain Structures** Reactivity to perineural cell layers of the arachnoid envelope surrounding the optic nerve was noted in 12 of 20 El Bagre-EPF patients, versus no controls ( $p<0.005$ ). This reactivity was not seen in the FS patients. The reactivity colocalized exactly with the antibodies to DPI, DPII, and ARVCF. Colocalization was also present in nearby vessels with p0071 by both IIF and CFM ( $p<0.005$ ). In 12 of 20 El Bagre-EPF patients and in one of 20 controls from the endemic area (a brother of one El Bagre-EPF patients), autoreactivity was noted surrounding brain cisternae, colocalizing with the arachnoid envelope of the optic nerve (mainly, but some reactivity was seen inside the nerve) and with the brain gyral and the sulci surfaces ( $p<0.005$ ). This reactivity was not seen in the FS patients, neither in control out of the endemic area (Figs. 1, 2, 3, 4, and 5).

**Neuropsychological and Behavioral Performance** Seventy percent of the El Bagre-EPF and three of five FS patients displayed neurological alterations that were statistically significantly higher in comparison with the other controls (i.e., symptoms of depression, anxiety, insomnia, and restlessness;  $p<0.005$ ). Intellectual sequelae (mainly alteration of executive function and constructional praxis) were not found to be different between patients and controls. Conversely, the kinesiological alterations and the burning sensation on the skin were present in 100% of the El Bagre-EPF and in three of five FS patients compared to none of the controls neither inside or outside the endemic area ( $p<0.005$ ). Autonomic alterations were also higher in the El Bagre-EPF patients ( $p<0.005$ ), including urinary incontinence, itching, burning sensations, esophageal dysmotility, and sphincter relaxation. Pupillary and other reflexes were normal, as well as testing for cranial nerves (II–XII), and non-statistical differences were found in comparison with the controls. Numbness, paresthesias, sensitivity to pressure, cold, heat and pain, bedside orthostatic hypotension, valsalva ratio, and beat-to-beat blood pressure show no differences either.

The NHP analysis showed higher depression among the El-Bagre-EPF patients (100%), in contrast to the controls from the endemic area (10%;  $p<0.005$ ). Postural deformities in the flexor tonus (as well as joint ankylosis and muscular weakness) were present in 70% of the El Bagre-EPF and in three of five FS patients, which was statistically significant to controls (5%;  $p<0.0005$ ).

Figure 1 shows a series of DIF, IIF, CFM, and IHC images, demonstrating by multiple techniques the autoreactivity of the El Bagre-EPF patient sera against PC and optic nerve envelope. Autoreactivity to PC in El Bagre-EPF patients is shown ( $\times 100$  for Fig. 1a and  $\times 400$  for Fig. 1c, d). Figure 1a shows positive staining to PC using rhodamine-conjugated goat anti-human IgG/IgM/IgA antiserum (blue

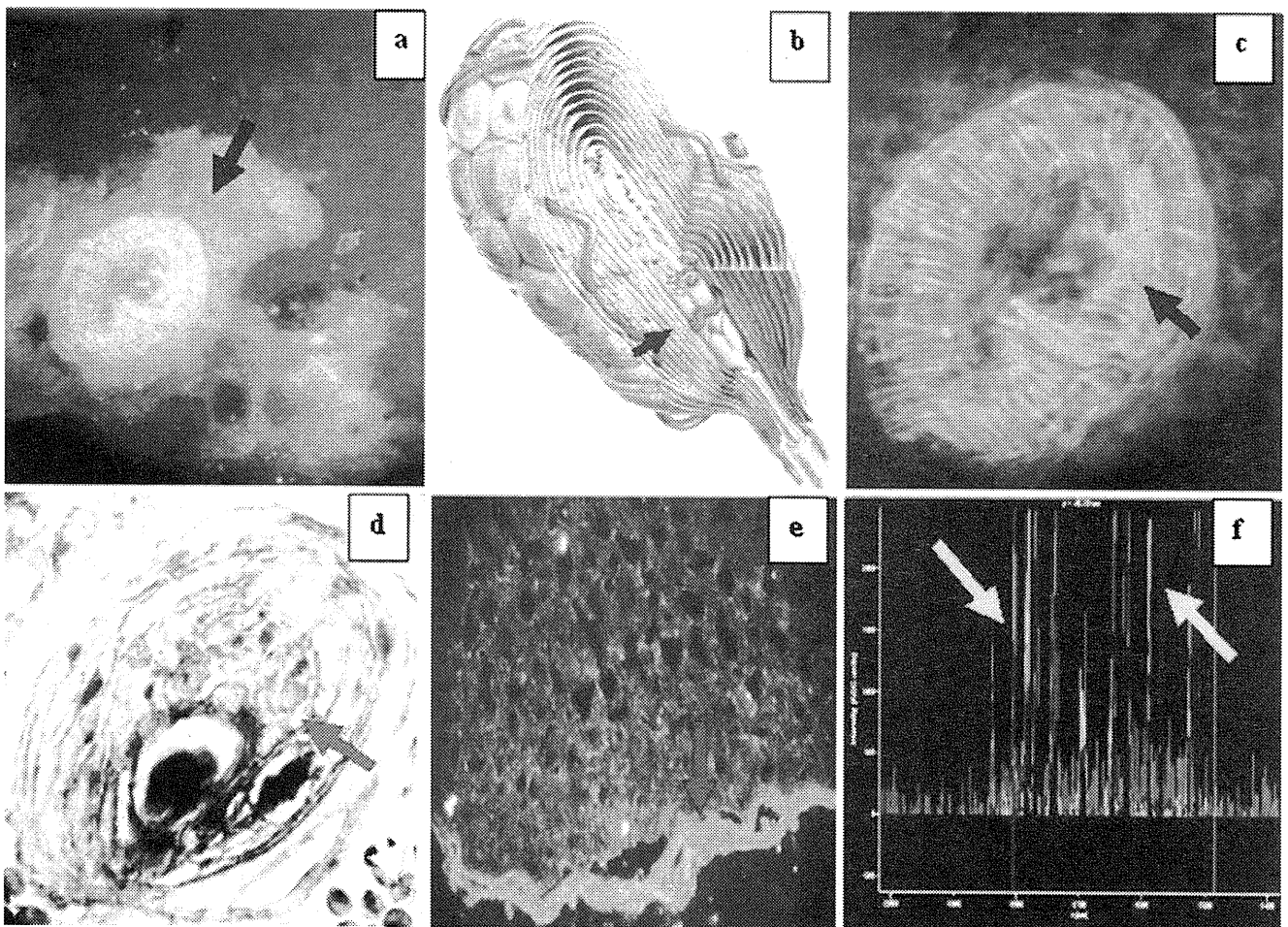


**Fig. 1** A series of IIF, DIF, IHC, and NDIC images demonstrating by multiple techniques the autoreactivity of the El Bagre-EPF patient sera against the PC and optic nerves

arrow, orange stain). Figure 1b is a cover picture of a PC, reproduced with permission from SKF 26, and GDAS (Ratingen, Germany). Figure 1c is the higher magnification of Fig. 1a ( $\times 400$ ; blue arrow), but in this case using anti-human IgG/IgM/IgA, conjugated with FITC (reactivity in green; blue arrow). Nomarski differential interference contrast confocal microscopy (NDIC) demonstrate that these structures were PC (data not shown). In Fig. 1c, IHC stains on El Bagre-EPF biopsies confirms the reactivity to PC (blue arrows) with anti-human IgM and IgA (dark brown stain onion shape stain, red arrow). Figure 1d is the IIF of a representative picture of a rat optic nerve, showing reactivity in the perineural meningeal sheaths recognized by El Bagre-EPF FITC conjugated anti-human IgG FITC conjugated antibodies (red arrow, green staining). In some cases, delicate intra-optic nerve reactivity was also seen (not shown). No controls were positive. Using CFM, we were able to show that El Bagre-EPF patients reactivity colocalized with anti-P0071 antibodies (data not shown). In Fig. 1e, CFM shows a colocalization with antibodies to DP I and II (red panel) with the El

Bagre-EPF autoantibodies (green panel). The blue peak is Dapi nuclear counterstain. The combined pikes colocalizing are pointed by the yellow arrows.

*El Bagre-EPF Patient Sera Reactive Against Some Peripheral Nerves* In Fig. 2 DIF, IIF, and IHC revealed autoreactivity against peripheral nerves. Figure 2a, c, d DIF reveals autoreactivity to peripheral nerve bundles, some directed against the epineurium, perineurium, and endoneurium. In Fig. 2a, the black arrows show positivity inside and in the periphery of the nerve with antibodies to IgG-FITC conjugated from one El Bagre-EPF patient (yellowish-green stain); the red stain (blue arrows) is PP9.5 stain to show colocalization of El Bagre-EPF antibodies with neural components (Fig. 2b). El Bagre-EPF sera shows reactivity to peripheral nerves using FITC conjugated anti-human IgG/IgA/IgM polyclonal antibodies (black arrows) (green staining). Figure 2c is similar as Fig. 2a, but at  $\times 100$ . Figure 2d shows H&E stain demonstrating a strong lymphohistiocytic infiltrate around one of the El Bagre-EPF dermal nerves and edema (blue arrows). Figure 2e shows IHC positive for

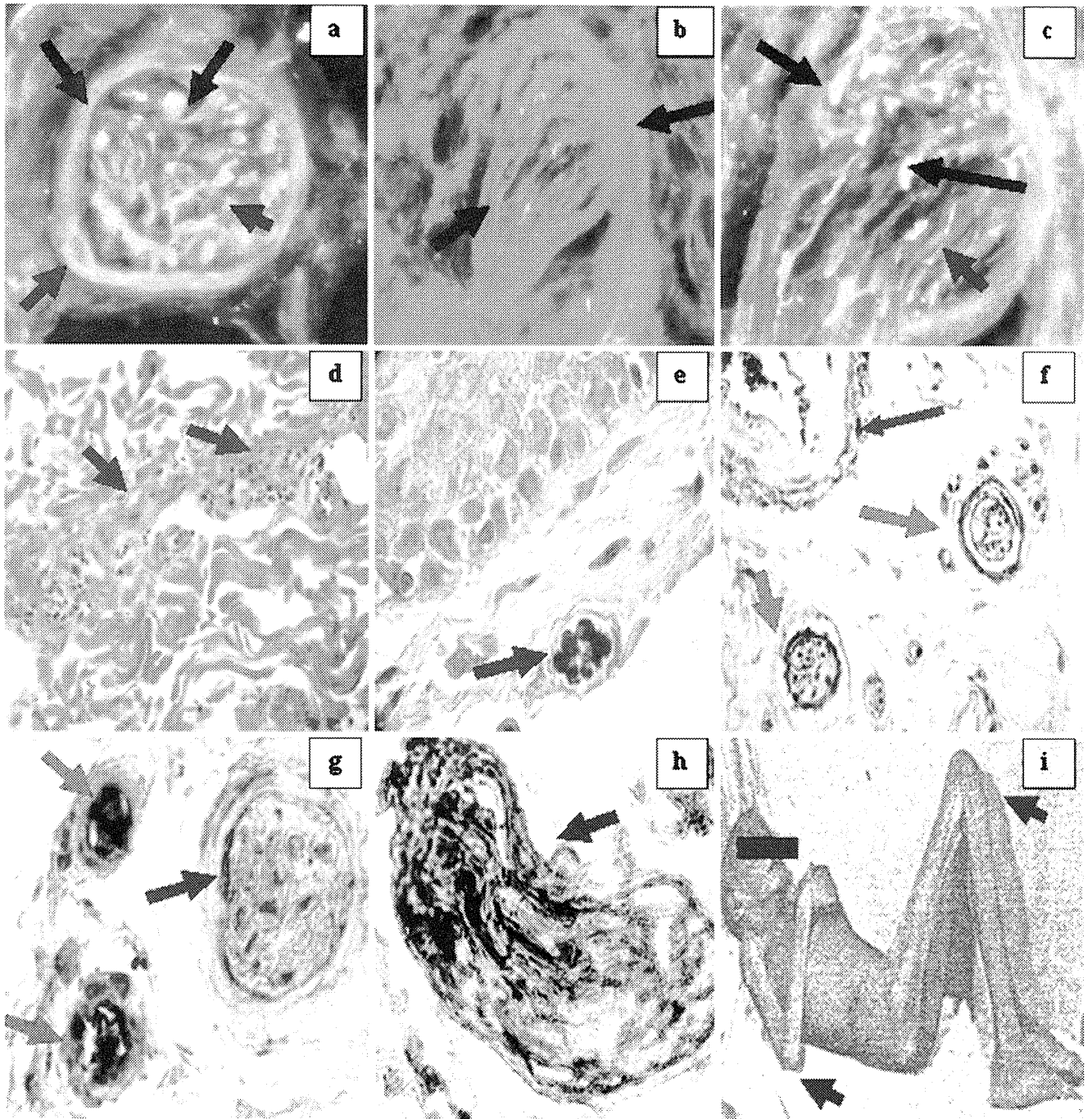


**Fig. 2** A series of IIF, DIF, and IHC images demonstrating the autoreactivity of the El Bagre-EPF patient sera against several peripheral nerves

anti-human S-100 in nerves (blue arrow). Figure 2g shows nerve positivity with anti-human IgA (blue arrow) and positivity to two vessel (red arrows). Figure 2h demonstrates strong staining of a nerve with anti-human IgM antibody (blue arrow; brown staining). Figure 2i shows the “pose of pemphigus” with dorsiflexion of extremities (blue arrows). By IIF, 11 of the 20 El Bagre-EPF sera showed nerve reactivity to the thin nerves, especially to their

epineurium, perineurium, endoneurium, and to vessels around and inside the nerve bundles. El Bagre-EPF patient antibodies colocalized with neural markers demonstrated by DIF, IIF, and IHC; positivity with S-100, NSE, PPG 9.5, GFAP, CD57, and neurofilament supports the neural origin of these antigens. The autoantibodies in El Bagre-EPF were polyclonal; thus, nine of the 20 samples tested positive to thin nerves utilizing anti-